Supplementary Material for CrystEngComm

A Predicted Dimer-based Polymorph of 10,11-Dihydrocarbamazepine (Form IV)

Jean-Baptiste Arlin, Andrea Johnston, Gary Miller, Alan R. Kennedy, Sarah L. Price and Alastair J. Florence*

Electronic Supplementary Information

1. Crystallisation details, results and multi-sample XRPD analysis

Details of the conditions used for the 71 automated parallel crystallisations are listed in Table S1 alongside the corresponding outcomes for each crystallisation and are also presented in graphical form in Figure S1. Details of each of the 99 manual solution recrystallisations are given in Tables S2a and S2b.

A small quantity (1 - 50 mg) of each recrystallised sample was analyzed using transmission foil XRPD data collected on a Bruker AXS D8-Advance transmission diffractometer equipped with θ/θ geometry, primary monochromated radiation (Cu $K\alpha_1$, λ = 1.54056 Å), a Braun 1D position sensitive detector (PSD) and an automated multi-position *x*-*y* sample stage (Florence *et. al.*, 2003). Samples were mounted on a 28 position sample plate supported on a polyimide (Kapton, 7.5 μm thickness) film. Data were collected from each sample in the range 4 – 35 ^{o} 2θ with a 0.015 ^{o} 2θ step size and 1 sec. step^{-1} count time (data collection time per sample *ca*. 45 mins). Samples were oscillated ± 0.5 mm in the *x*-*y* plane at a speed of 0.3 mm sec.$^{-1}$ throughout data collection to maximize particle sampling and minimize preferred orientation effects.

Table S3 lists the published unit cells for each fully characterised form obtained from the crystallisation search and representative XRPD data, that have been Pawley fitted to the cells listed in Table S3, are shown in Figure S2. It should be noted that pure form III was not obtained from the crystallisation search, but was identified from a single-crystal analysis of a mixed phase sample and hence is not included in Figure S2. The refined room temperature lattice parameters obtained from each fit are also presented, observed differences between these and those parameters listed in Table S3 can be attributed to differences in data collection temperature.

Trifluoroacetic acid and butyric acid solvates were characterised by XRPD and DSC/TGA. Only limited single crystal diffraction data were collected for the trifluoroacetic acid solvate due to the poor diffraction quality of the samples obtained during the study. Although the structure is not of publication quality, the limited information obtained provided confirmation that the structure adopts an $R^2_2(8)$ heterodimer DHC:trifluoroacetic acid packing motif. Further attempts to obtain a publication quality structure are ongoing. No suitable single crystal samples were obtained for the butyric acid sample, attempts at structure determination from X-ray powder diffraction data are ongoing.

* Alastair.florence@strath.ac.uk

Table S1: Automated crystallisation experiments; 4ml solvent were added to ~200mg of DHC, solutions were heated to $T_{prep,}$ filtered and then crystallisation was induced by cooling. Solutions that did not crystallise within 24hours were transferred to vials for solvent evaporation at RT.

Sample identifier	Solvent 1	T_{prep} (°C)	T_{cool} (°C)	Vortex (rpm)	Form
004000	pentane-1,5-diol	145	25	1000	I
004001	1-methylnapthalene	145	25	1000	I / II
004002	2-phenylethanol	145	25	1000	II
004003	n-dodecane	145	25	1000	I
004004	nitrobenzene	145	25	1000	I
004005	1-methyl-2-pyrrolidinone	145	25	1000	II
004006	octan-1-ol	145	25	1000	I
004007	DMSO	145	25	1000	I / II
004008	aniline	145	25	1000	II
004009	octan-2-ol	145	25	1000	I / II
004010	2-butoxyethanol	145	25	1000	II
004011	DMA	145	25	1000	II
004012	furfural	145	25	1000	0
004013	2-methoxyethylether	145	25	1000	I / II
004014	cyclohexanol	145	25	1000	I / II
004015	hexan-1-ol	145	25	1000	I
004016	anisole	110	25	1000	I/II
004017	pentyl acetate	110	25	1000	I/II
004018	butyl ether	110	25	1000	I/II
004019	xylene	110	25	1000	I/II
004020	pentan-1-ol	110	25	1000	I
004021	2-ethoxyethanol	110	25	1000	II
004022	3-methylbutan-1-ol	110	25	1000	I
004023	DMF	110	25	1000	I / II
004024	butylacetate	110	25	1000	I / II
004025	diethylcarbonate	110	25	1000	I/II
004026	2-methoxyethanol	110	25	1000	II
004027	tetrachloroethene	110	25	1000	II
004028	acetic acid	110	25	1000	S
004029	pentan-2ol	110	25	1000	I / II
004030	4-methyl-2-pentanone	110	25	1000	I
004031	butan-1-ol	110	25	1000	I
004032	isobutylacetate	75	25	1000	II
004033	pyridine	75	25	1000	II

Sample identifier	Solvent 1	T_{prep} (°C)	T_{cool} (°C)	Vortex (rpm)	Form
004034	toluene	75	25	1000	II
004035	2-methylpropan-1-ol	75	25	1000	I
004036	1,4-dioxan	75	25	1000	II
004037	nitromethane	75	25	1000	I/II
004038	iso-octane	75	25	1000	I/II
004039	water	75	25	1000	0
004040	n-heptane	75	25	1000	I/II
004041	butan-2-ol	75	25	1000	I
004042	propan-1-ol	75	25	1000	I
004043	triethylamine	75	25	1000	I/II
004044	trichloroethylene	75	25	1000	I/II
004045	1,2-dimethoxyethane	75	25	1000	II
004046	dichloroethane	75	25	1000	I/II
004047	propan-2-ol	75	25	1000	I
004048	acetonitrile	45	25	1000	I / II
004049	cyclohexane	45	25	1000	I / II
004050	benzene	45	25	1000	II
004051	methylethylketone	45	25	1000	I / II
004052	1-chlorobutane	45	25	1000	II
004053	ethanol	45	25	1000	I
004054	ethylacetate	45	25	1000	II
004055	carbon tetrachloride	45	25	1000	II
004056	hexane	45	25	1000	I / II
004057	THF	45	25	1000	II
004058	chloroform	45	25	1000	I / II
004059	methyl acetate	45	25	1000	II
004060	tert-butyl methyl ether	45	25	1000	I / II
004061	cyclopentane	45	25	1000	II
004062	methanol	45	25	1000	II
004063	acetone	45	25	1000	II
004064	formamide	145	25	1000	S
004065	formic acid	75	25	1000	S
004066	trifluoroethanol	75	25	1000	II
004167	butyric acid	145	25	1000	S
004168	trifluoroacetic acid	65	25	1000	S
004169	dichloromethane	30	25	1000	0
004170	diethylether	30	25	1000	0

Key

0 = insufficient sample obtained for analysis
I = form I
II = form II
S = solvate formed

Figure S1. Score plot of the two principal components from PCA analysis of 15 observed and calculated solvent properties shown with an ellipse that represents the Hotelling T2 with 95% confidence. The position of each point is determined by the PCA scores t1 and t2 and are coloured according to crystallization outcome; green diamond-form I, blue diamond form II, orange diamond mixed forms I and II, red triangle – solvate and black cross-insufficient material for analysis. The key to identify solvents is provided at the bottom.

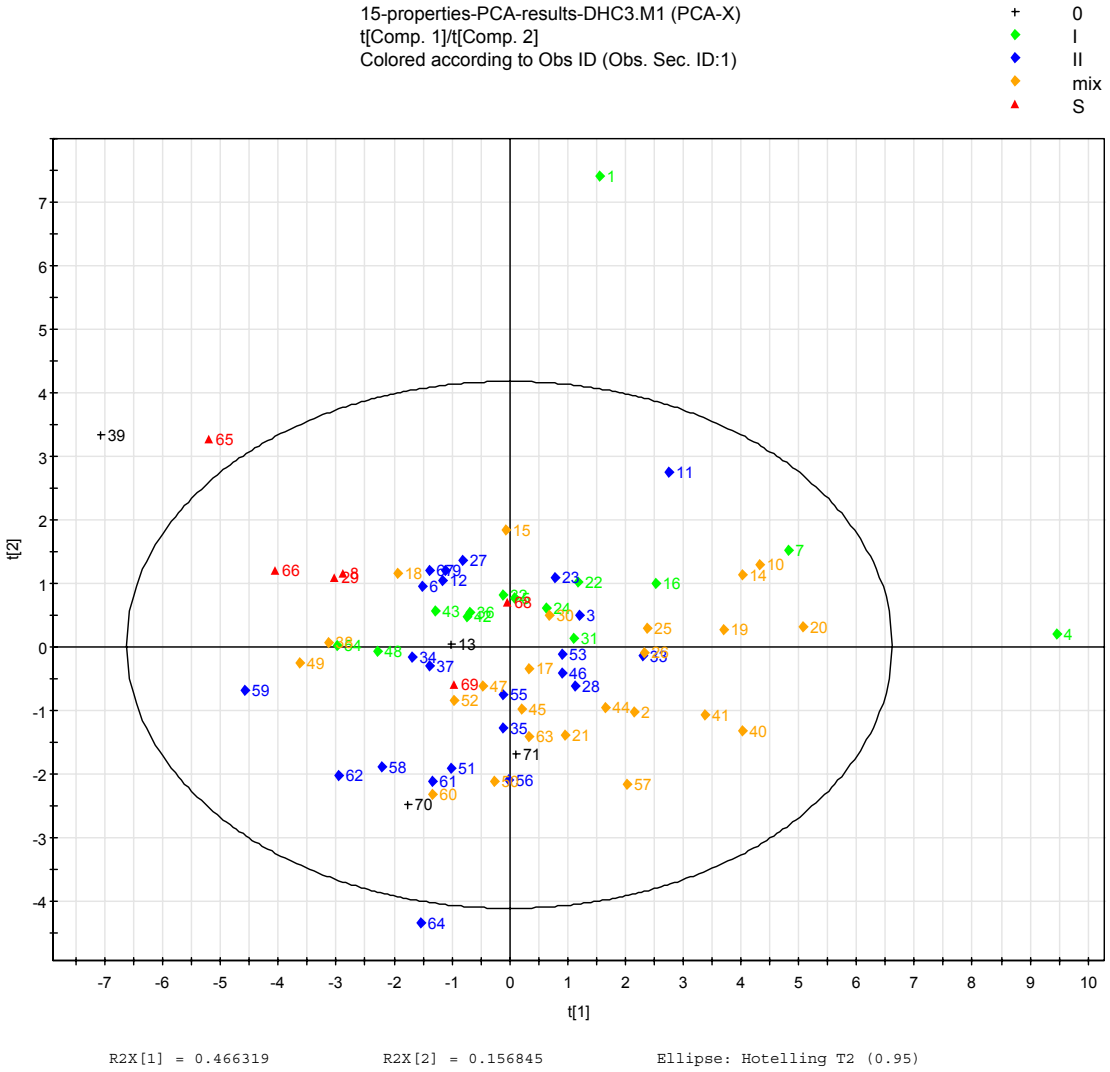

Solvent key:

ID	Solvent	ID	Solvent	ID	Solvent
1	1,5-pentanediol	24	3-methyl-1-butanol	47	1,2-dichloroethane
2	1-methylnapthalene	25	Butylacetate	48	2-propanol
3	2-phenylethanol	26	Diethyl carbonate	49	Acetonitrile
4	Dodecane	27	2-methoxyethanol	50	Cyclohexane
5	Nitrobenzene	28	Tetrachloroethene	51	Benzene
6	*N*-methyl-2-pyrrolidone	29	Ethanoic acid (acetic acid)	52	2-butanone
7	1-octanol	30	2-pentanol	53	1-chlorobutane
8	dimethylsulphoxide (DMSO)	31	4-methyl-2-pentanone	54	Ethanol
9	Aniline	32	1-butanol	55	Ethylacetate
10	2-octanol	33	Isobutyl acetate	56	Carbon tetrachloride
11	2-butoxyethanol	34	Pyridine	57	Hexane

12	*N,N*-dimethylacetamide (DMA)	35	Toluene	58	Tetrahydrofuran (THF)
13	Furfural	36	2-methyl-1-propanol	59	Methanol
14	2-methoxyethylether	37	1,4-dioxane	60	Chloroform
15	Cyclohexanol	38	Nitromethane	61	Methyl acetate
16	1-hexanol	39	Water	62	Acetone
17	Anisole	40	2,2,4-trimethylheptane	63	2-methoxy-2-methylpropane
18	*N,N* dimethylformamide (DMF)	41	Heptane	64	Cyclopentane
19	Pentylacetate	42	2-butanol	65	Formamide
20	Butylether	43	1-propanol	66	Methanoic acid (formic acid)
21	Xylene	44	Triethylamine	67	Trifluoroethanol
22	1-pentanol	45	Trichloroethylene	68	Butyric acid
23	2-ethoxyethanol	46	1,2-dimethoxyethane	69	Trifluoroacetic acid
70	dichloromethane	71	diethylether		

Table S2a: Manual crystallisation experiments; solutions were saturated at T_{prep} and crystallisation was induced by cooling/solvent evaporation at temperatures indicated by T_{cool} .

Sample identifier	Solvent	Solvent volume (ml)	T_{prep} (°C)	T_{cool} (°C)
004067	water	3	60	25
004068	water	3	60	25
004069	water	3	60	25
004070	acetone	3	35	25
004071	acetone	3	35	25
004072	acetone	3	35	25
004073	DMSO	3	25	25
004074	DMSO	3	25	25
004075	DMSO	3	25	25
004076	dioxane	3	25	25
004077	dioxane	3	25	25
004078	dioxane	3	25	25
004079	DMF	3	25	25
004080	DMF	3	25	25
004081	DMF	3	25	25
004082	furfural	3	25	25
004083	furfural	3	25	25
004084	furfural	3	25	25
004085	trifluoroethanol	3	25	25
004086	trifluoroethanol	3	25	25
004087	trifluoroethanol	3	25	25
004088	water	3	60	5
004089	water	3	60	5
004090	water	3	60	5
004091	acetone	3	35	5
004092	acetone	3	35	5
004093	acetone	3	35	5
004094	DMSO	3	25	5
004095	DMSO	3	25	5
004096	DMSO	3	25	5
004097	dioxane	3	25	5
004098	dioxane	3	25	5
004099	dioxane	3	25	5
004100	DMF	3	25	5
004101	DMF	3	25	5
004102	DMF	3	25	5
004103	furfural	3	25	5
004104	furfural	3	25	5
004129	furfural	3	25	5
004105	trifluoroethanol	3	25	5
004106	trifluoroethanol	3	25	5
004107	trifluoroethanol	3	25	5
004108	water	3	60	0
004109	water	3	60	0
004111	acetone	3	35	0
004112	acetone	3	35	0
004114	DMSO	3	25	0
004115	DMSO	3	25	0

Table S2a continued

Sample identifier	Solvent	Solvent volume (ml)	T_{prep} (°C)	T_{cool} (°C)
004117	dioxane	3	25	0
004118	dioxane	3	25	0
004120	DMF	3	25	0
004121	DMF	3	25	0
004123	furfural	3	25	0
004124	furfural	3	25	0
004126	trifluoroethanol	3	25	0
004127	trifluoroethanol	3	25	0
004130	DMA	3	25	25
004131	DMA	3	25	25
004132	DMA	3	25	25
004133	nitromethane	3	25	25
004134	nitromethane	3	25	25
004135	nitromethane	3	25	25
004136	NMP	3	25	25
004137	NMP	3	25	25
004138	NMP	3	25	25
004139	DMA	3	25	5
004140	DMA	3	25	5
004141	DMA	3	25	5
004142	nitromethane	3	25	5
004143	nitromethane	3	25	5
004144	nitromethane	3	25	5
004145	NMP	3	25	5
004146	NMP	3	25	5
004147	NMP	3	25	5
004148	DMA	3	25	0
004149	DMA	3	25	0
004151	nitromethane	3	25	0
004152	nitromethane	3	25	0
004154	NMP	3	25	0
004155	NMP	3	25	0
004157	butyric acid	3	25	25
004157b	butyric acid	1	25	25
004157c	butyric acid	1	25	25
004163	trifluoroacetic acid	3	25	25
004163b	trifluoroacetic acid	1	25	25
004163c	trifluoroacetic acid	1	25	25
004158	butyric acid	3	25	5
004158b	butyric acid	1	25	5
004158c	butyric acid	1	25	5
004164	trifluoroacetic acid	3	25	5
004164b	trifluoroacetic acid	1	25	5
004164c	trifluoroacetic acid	1	25	5
004171	butyric acid	1	25	0
004171b	butyric acid	1	25	0
004172	trifluoroacetic acid	1	25	0
004172b	trifluoroacetic acid	1	25	0
004173	methanol	3	25	25
004174	methanol	3	25	25
004175	methanol	3	25	25

Table S2b: Physical forms, identified by XRPD, from each solvent and condition listed in Table S2a.

Solvent	Tcool = 25			Tcool = 5			Tcool = 0	
	R1	R2	R3	R1	R2	R3	R1	R2
Water	0	0	0	0	0	0	0	0
Acetone	II	II	I / II	II	II	II	I / II	I / II
DMSO	I / III	I / II	I / II	II	II	II	S	S
Dioxane	I / II	I / II	I / II	II	I / II	I	I	I
DMF	II	II	II	II	II	II	I / II	I / II
Furfural	0	0	I	0	II	0	0	0
TFE	II	II	II	I / II	II	II	I	I / II
DMA	II	II	II	I / II	I / II	I / II	0	I / II
Nitromethane	II	II	II	II	I / II	II	I / II	I / II
NMP	II	II	II	II	II	II	I / II	I / II
Butyric acid	I / II / S	0	0	S	0	0	0	0
Trifluoroacetic acid	S	0	0	S	0	0	0	0
Methanol	I / II	I / II / III	I / II	-	-	-	-	-

Key
0 = insufficient sample obtained for analysis; I = form I; II = form II; S = solvate formed; - = no crystallisation.

Table S3. Summary of unit cell parameters for each form of DHC obtained during the crystallisation search.

.

Crystal Form	**T (K)**	***a* (Å)**	***b* (Å)**	***c* (Å)**	**α (°)**	**β (°)**	**γ (°)**	**Volume (Å^3)**	**Spacegroup**
Form I (monoclinic) [1]	294	5.505(1)	9.158 (2)	24.266 (7)	90.0	95.95 (2)	90.0	1216.775	$P2_1/c$
Form II (orthorhombic) [2]	120	9.0592 (4)	10.3156 (5)	25.053 (12)	90.0	90.0	90.0	2341.27(19)	*Pbca*
Form III (triclinic) [3]	150	5.4233 (12)	9.200 (5)	24.189 (6)	87.59(3)	84.23(2)	88.93(3)	1199.6(8)	$P\bar{1}$
Formic acid [4]	123	5.2298 (4)	9.3849(12)	14.4858 (18)	83.853 (5)	88.230 (7)	88.221 (7)	706.28	$P\bar{1}$
Acetic acid [5]	123	5.3104 (4),	15.424(17)	18.732(2)	90.0	95.65(1)	90.0	1528.3(3)	$P2_1/c$
Trifluoroacetic acid [6]	298	27.670 (10)	5.5184 (10)	23.009 (8)	90.0	113.962 (4)	90.00	3210.6(2)	$P2_1/a$
DMSO solvate [7]	123 (2)	10.296(3)	6.8543 (2)	23.3599(6)	90.0	98.932(2)	90.00	1624.639(8)	$P2_1/c$
Formamide [8]	120 (2)	8.4690(4)	9.0215(4)	10.3137(4)	74.363(3)	83.63(3)	70.8473(3)	716.61 (5)	$P\bar{1}$

[1] Bandoli, G., Nicolini, M., Ongaro, A., Volpe, G. & Rubello, A. (1992). *J. Chem. Crystallogr.* **22**, 177–183; [2] Harrison, W. T. A., Yathirajan, H. S. & Anilkumar, H. G. (2006). *Acta Cryst.* C**62**, o240–o242; [3] Leech, C. K., Florence, A. J., Shankland, K., Shankland, N. & Johnston, A. (2007). *Acta Cryst.* **E63**, o675-o677; [4] Johnston, A., Florence, A. J., Fernandes, P., Shankland, N., Kennedy, A. R. (2007) *Acta Cryst.* **E63**, o1469-o1470; [5] Johnston, A., Florence, A. J., Fernandes, P., Shankland, N., Kennedy, A. R. (2006) *Acta Cryst.* **E62**, o5361-o5362; [6]unpublished data; [7]Johnston, A., Florence, A. J., Shankland, K., Leech, C. K., Shankland, N., Fernandes, P., (2007) *Acta Cryst.* **E63**, o3918-o3919; [8] Johnston, A., Florence, A. J., Fernandes, P., Shankland, N., Kennedy, A. R. (2007) *Acta Cryst.* **E63**, o3888-o3889.

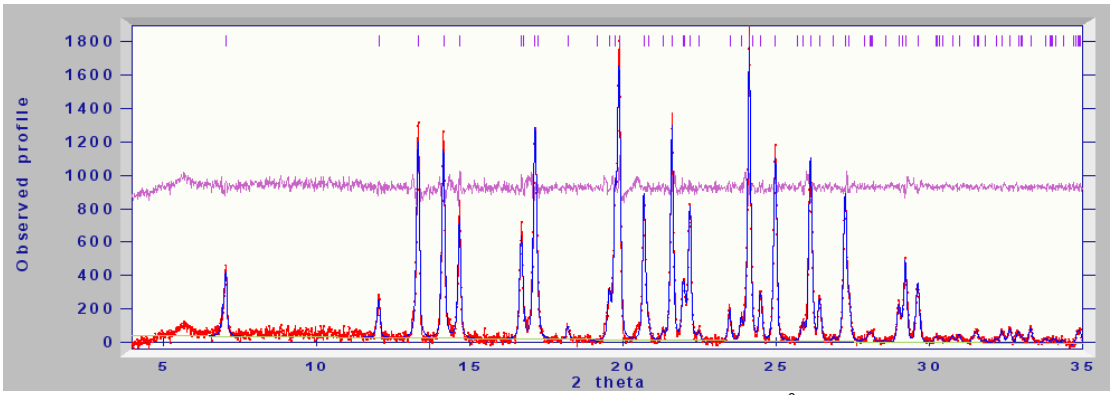

Figure S2(a) DHC Form I. Refined cell parameters = *a*, *b*, *c* (Å) = 5.5283, 9.175, 24.314; α, β, γ (°) = 90.0, 96.141, 90.0 Pawley χ^2 = 3.589.

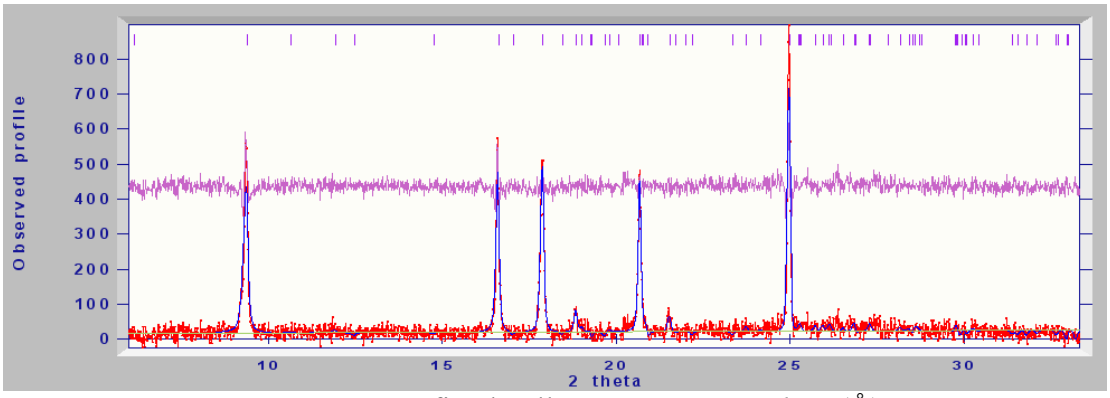

Figure S2(b) DHC Form II. Refined cell parameters = *a*, *b*, *c* (Å) = 9.058, 10.558, 24.964; α, β, γ (°) = 90.0, 90.0, 90.0 Pawley χ^2 = 2.069.

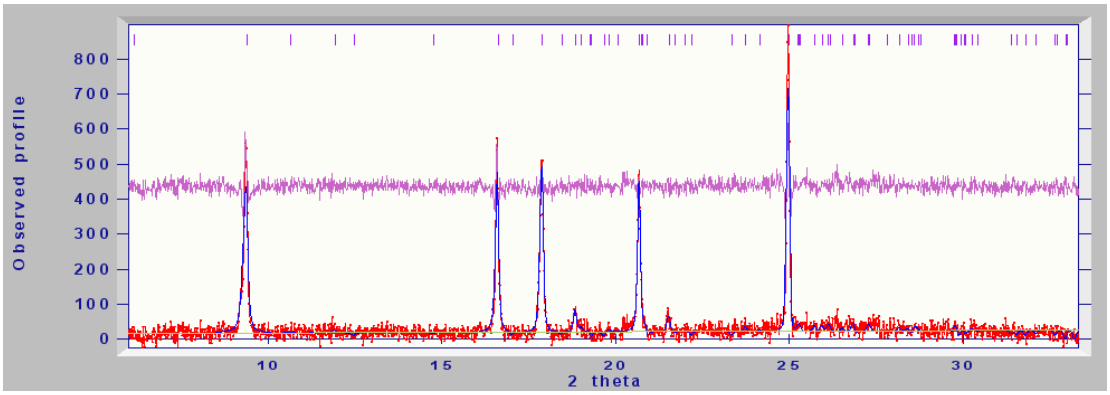

Figure S2(c) DHC-Formic acid. Refined cell parameters = *a*, *b*, *c* (Å) = 5.158, 9.318, 14.105; α, β, γ (°) = 82.961, 87.10, 87.857 Pawley χ^2 = 1.428.

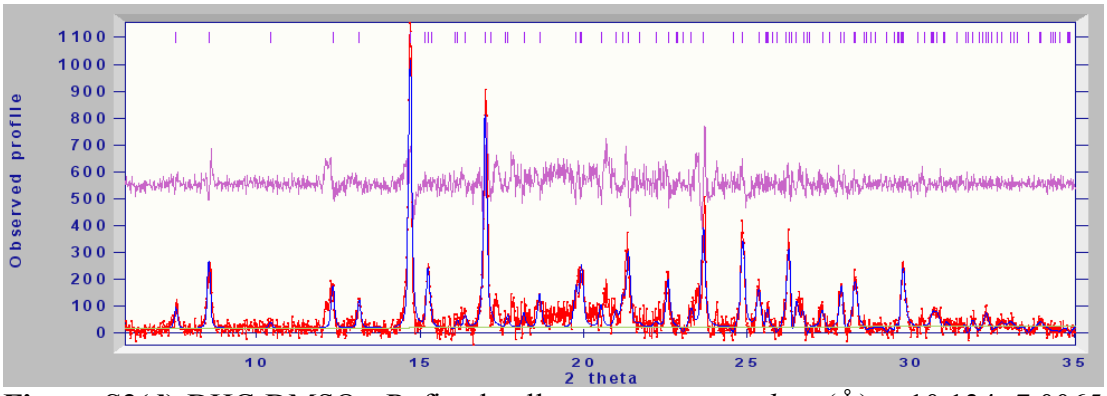

Figure S2(d) DHC-DMSO. Refined cell parameters = *a*, *b*, *c* (Å) = 10.134, 7.0065, 23.625; α, β, γ (°) = 90.0, 99.578, 90.0. Pawley χ^2 = 2.101.

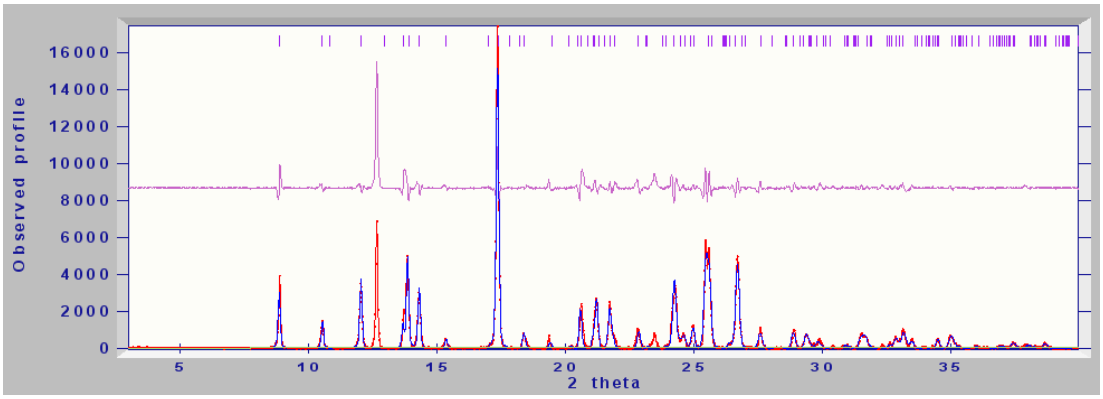

Figure S2(e) DHC-formamide. Refined cell parameters = *a*, *b*, *c* (Å) = 8.518, 9.0166, 10.31008; α, β, γ (°) = 74.85, 83.392, 73.636. Pawley χ^2 = 28.52.

Desolvation of DMSO solvate

The DMSO solvate was heated *in situ* in a 0.7mm borosilicate capillary above 85°C and the pattern identified as form I via a Pawley type fit to the known crystal lattices and space groups. This is consistent with STA data that showed an endothermic event with simultaneous weight loss at 85 °C followed by a final endotherm at 202.5 °C consistent with the melting point of form I.

Recrystallisation from the Melt

A sample of DHC was loaded into a 0.7mm borosilicate and heated to just above the melting point on a Bruker-AXs D8 X-ray powder diffractometer using an Oxford Cryosystems Crysostream 700 Plus system. The sample immediately melted and recrystallized. XRPD data collected from the recrystallized sample confirmed that the sample had degraded to produce 10,11-dihydro-5H-dibenzo[b,f]azepine (Reboul et al., 1980).

2. Computational Method

The molecular structure was optimized at the MP2 6-31G(d,p) level, using GAUSSIAN, and starting from both syn and anti conformations. The energy difference between these conformational minima, ΔE_{intra}, equals 1.70 kJ mol^{-1}, and contributes to the lattice energy as these conformations were held rigid. A search for possible crystal structures was performed using MOLPAK (Holden *et.al.*, 1993) to generate densely packed structures in common coordination types with Z'=1. These structures were lattice energy minimized using DMAREL,(Willock *et.al.,* 1995) where the intermolecular lattice energy, U_{inter}, was calculated from the distributed multipole representation of the wavefunction and an atom-atom exp-6 potential with the FIT parameters.(Coombes, 1996). The unique low energy structures are given in Table S4, ordered by the Intermolecular Lattice Energy, U_{inter}. Figure S3 displays the crystal energy landscape in terms of the lattice energy, $E_{latt} = U_{inter} + \Delta E_{intra}$, noting that the relative energies of the structures containing the syn and anti conformations are rather sensitive to the ab initio method used to calculate ΔE_{intra}. The second derivatives of the lattice energy were used to estimate the zero point and thermal energies at 298 K, providing as estimate of the relative free energies (Anghel *et. al.*, 2002). These free energies reorder Forms I and II. Form IV of dihydrocarbamazepine is 7.5, 9.2, and 8.6 kJ mol^{-1} less stable than the most stable structure in terms of intermolecular lattice energy, lattice energy including the conformational energy penalty, ΔE_{intra}, and free energy, respectively.

This approximate energy landscape was produced in 2007, and the unique structures in the lowest 10 kJ mol^{-1} stored on the STFC e-Science centre dataportal and are available from the authors on request.

Table S4: The crystal energy landscape of the lowest energy structures of DHC, within 10 kJ mol^{-1} of the global minimum in total lattice energy.

Label	Conformer	Motif	Space Group	Cell Parameters						Density (g/cm3)	Lattice Energies (kJ/mol)		Estimated Energy at 298K
				a(Å)	b(Å)	c(Å)	α(°)	β(°)	γ(°)		Intermolecular (U_{inter})	Total (E_{latt})	
cc46	anti	Catemer	Pbca	9.0927	10.7629	24.9555	90	90	90	1.30	-126.31	-126.31	-143.05
Form II VACTAU02[1]	**anti**	**Catemer**	**Pbca**	**9.0592(4)**	**10.3156(5)**	**25.0534(12)**	**90**	**90**	**90**				
fc13	syn	Catemer	P21/c	7.6193	7.6715	21.0792	90	89.587	90	1.28	-125.65	-123.95	-141.99
fc85	anti	Catemer	P21/c	5.5431	9.1955	24.3075	90	93.15	90	1.28	-125.52	-125.52	-144.06
Form I VACTAU01[2]	**anti**	**Catemer**	**P21/c**	**5.501(1)**	**9.158(2)**	**24.266(7)**	**90**	**95.95(2)**	**90**				
eo3*	anti	Catemer	P-1	5.5436	9.1954	24.6323	90	80.162	90	1.28	-125.51	-125.51	
Form III VACTAU03[3]	**anti**	**Catemer**	**P-1**	**5.4233(12)**	**9.200(5)**	**24.189(6)**	**87.59(3)**	**84.23(2)**	**88.93(3)**				
ca1	syn	Dimer	P-1	7.6825	7.4522	10.8595	85.305	90.49	87.237	1.28	-122.84	-121.14	-138.38
ak98	anti	Catemer	P21/c	12.9333	9.1116	10.6084	90	84.517	90	1.27	-122.74	-122.74	-139.44
ca121	syn	Dimer	P-1	11.113	7.7843	7.5835	102.577	80.979	96.351	1.26	-122.01	-120.31	-137.72
aj82	anti	Dimer	P2/c	11.8179	7.1837	15.8887	90	73.482	90	1.22	-121.18	-121.18	-140.32
ak61^	anti	Dimer	P21/c	14.3854	5.107	19.1661	90	63.452	90	1.26	-121.09	-121.09	-139.72
ai75	anti	Catemer	P21/c	11.3265	8.2388	13.4167	90	93.249	90	1.27	-121.08	-121.08	-139.99
af91	syn	Catemer	P21	7.7331	7.4092	10.8151	90	90.148	90	1.28	-121.03	-119.33	-137.20
bh107	anti	Catemer	Pca21	24.5911	5.4488	9.349	90	90	90	1.26	-120.95	-120.95	-140.18
ba51	syn	Catemer	P21	22.0619	7.5827	7.5819	90	90	90	1.25	-120.87	-119.17	-139.89
fc53	anti	Dimer	P21/c	7.9148	7.4419	21.6027	90	90.797	90	1.24	-120.76	-120.76	-140.29
fc2	syn	Catemer	P21/c	5.543	9.6467	23.2789	90	92.497	90	1.27	-120.43	-118.73	-137.95
fc59	syn	Catemer	P21/c	5.2669	10.1776	23.1635	90	89.114	90	1.27	-120.30	-118.60	-137.41
az38	anti	Catemer	P212121	24.9238	9.1765	5.535	90	90	90	1.25	-120.21	-120.21	-138.76
ab86	anti	Dimer	P-1	10.3272	8.0467	12.0287	95.368	111.921	44.639	1.26	-120.19	-120.19	-137.71
fc97	syn	Catemer	P21/c	10.4803	7.4687	15.9092	90	89.412	90	1.27	-120.05	-118.35	-136.26
ak128	syn	Catemer	P21/c	11.1887	8.0112	14.1639	90	94.223	90	1.25	-119.61	-117.91	-136.86
al104	anti	Dimer	P2/c	12.3744	7.1399	15.7685	90	111.69	90	1.22	-119.44	-119.44	-138.70
ca42	syn	Dimer	P-1	9.7149	5.0995	14.1636	90.427	107.163	69.366	1.27	-119.41	-117.71	-135.93
ab5	syn	Dimer	P-1	9.587	5.1141	13.1215	89.175	105.912	91.14	1.28	-119.26	-117.56	-135.69

ca5	anti	Dimer	P-1	9.4244	5.2268	13.3725	86.081	75.857	88.734	1.24	-119.07	-119.07	-138.57
de59	anti	Dimer	C2/c	22.1144	7.1912	15.76	90	97.156	90	1.27	-119.05	-119.05	-136.65
ca26	anti	Dimer	P-1	8.2155	7.2002	11.5134	89.352	85.109	108.133	1.23	-118.95	-118.95	-136.77
ak2	syn	Dimer	P21/c	13.8967	5.215	19.4301	90	117.130	90	1.26	-118.80	-117.10	-135.50
Form IV	**syn**	**Dimer**	**P21/c**	**13.207(6)**	**5.347(2)**	**18.891(7)**	**90**	**116.37(2)**	**90**				
am17	anti	Dimer	P21/c	7.1347	12.0959	14.969	90	99.517	90	1.24	-118.35	-118.35	-137.19
cb18	syn	Dimer	Pbca	7.4218	16.4408	21.7468	90	90	90	1.19	-118.01	-116.31	-139.47
ab25	anti	Dimer	P-1	7.6413	7.5219	11.1528	80.253	87.52	86.755	1.26	-117.77	-117.77	-136.32
de14	anti	Catemer	C2/c	26.0958	9.2288	26.9558	90	22.961	90	1.25	-117.49	-117.49	-133.83
ab9	anti	Catemer	P-1	10.1757	7.2641	12.1207	80.626	100.224	52.09	1.21	-117.40	-117.40	-136.13
af18	anti	Dimer	P21	5.4931	9.2157	13.6959	90	67.651	90	1.23	-117.40	-117.40	-135.62
de70	anti	Dimer	C2/c	24.0451	7.114	15.7068	90	107.012	90	1.23	-117.32	-117.32	-135.44

* Form III is Z'=2 and hence could not have been found in the search, or have the free energy estimated.
^ A structure whose packing is almost identical to that of form IV, except that it has the molecules in the anti conformation.
[1]Harrison *et. al.,* 2006; [2]Bandoli *et. al.,* 1992; [3]Leech *et. al.,* 2007

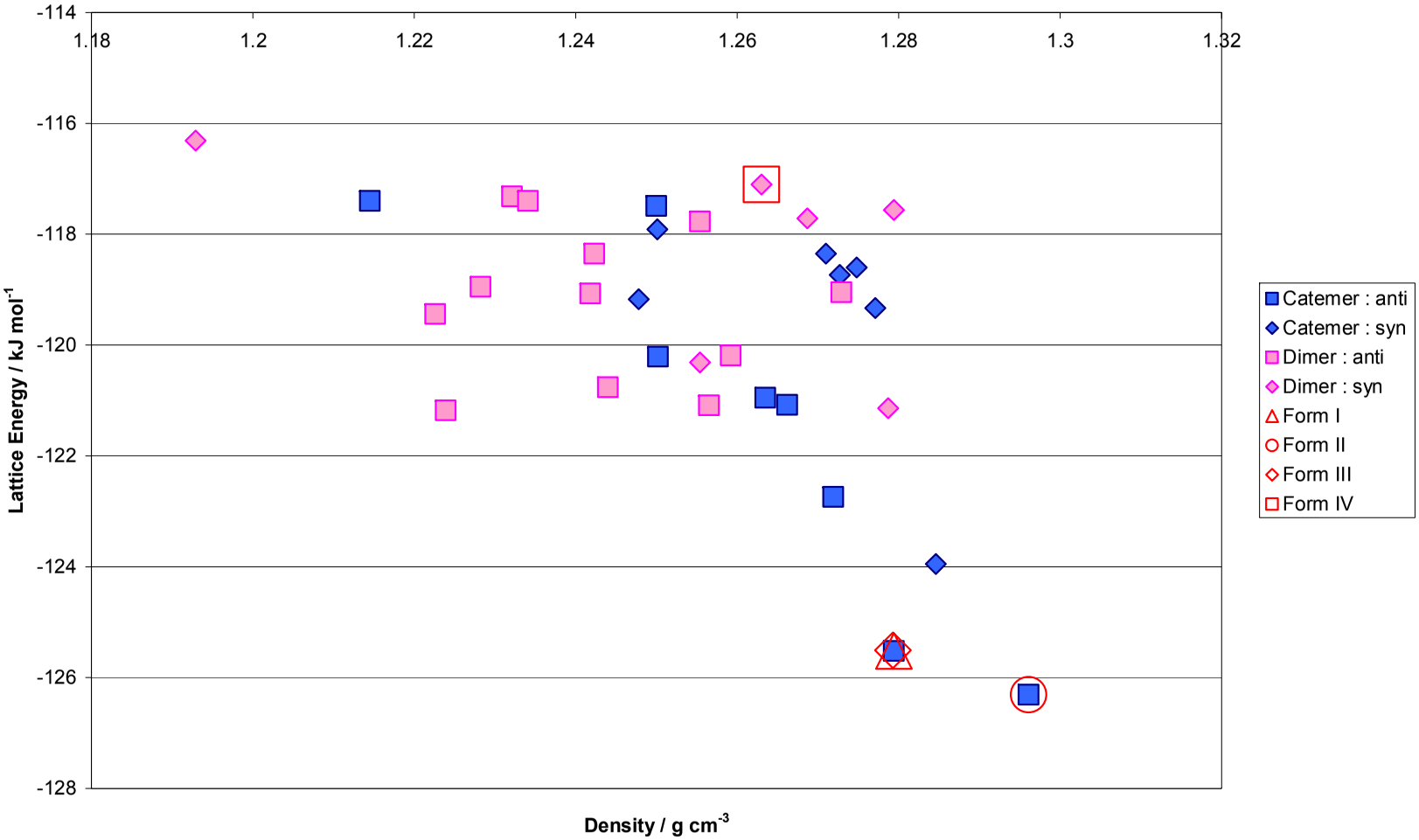

Figure S3. Crystal Energy Landscape of Dihydrocarbamazepine predicted structures.

3. XPac Analysis

Method

The packing arrangement of DHC form IV was compared to the three known forms using the xPac method. The molecular shape of the DHC molecule was parameterised using the same eight common ordered set of points utilised in a previous study as indicated with red circles in scheme S1. The calculations were performed using medium cut-off parameters to identify mean differences δ, 10˚ for δ_{ang} and 18° for δ_{tor} and δ_{dhd}. The structures examined are given in table S5.

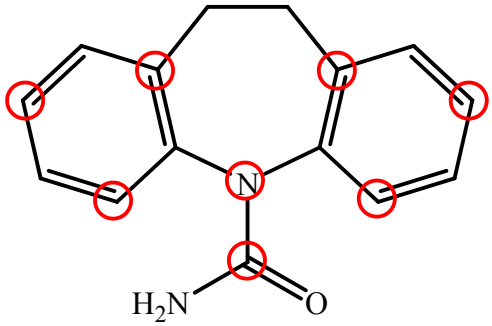

Scheme S1: COSPS selected for analysis.

Table S5: Details of structures examined.

Crystal		SpGr	Z'	CCDC	Ref
1	**DHC form I**	**P21/c**	**1**	**VACTAU01**	**3**
2	**DHC form II**	**Pbca**	**1**	**VACTAU02**	**4**
3	**DHC form III**	**P-1**	**2**	**VACTAU03**	**5**
4	**DHC form IV**	**P21/c**	**1**		**This work**

Results

The analysis shows that the structures of the polymorphs are based on two supramolecular constructs, a stack of molecules related by translation symmetry **A** (fig. S4). Construct **A** is a similar stacking arrangement described for carbamazepine structures by Gelbrich and Hursthouse and the occurrence of this construct is independent of the hydrogen bonding arrangement in the structures as it occurs in **1**, **3** and **4**.

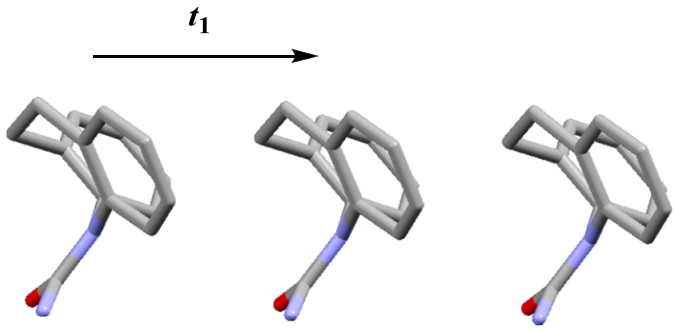

Figure S4: Stack **A** viewed approximately perpendicular to the translation vector $\boldsymbol{t}_1$.

Stack **A** is the basis of construct $\mathbf{A_1}$, which is composed of two antiparallel **A** stacks related by an inversion operation. In the case of **4** this construct results from the packing of stacks of hydrogen bonded *anti* dimers (Fig. S5a) while in **1** and **3** the alignment of the hydrogen bonded catamers along the vector $\boldsymbol{t}_1$ results in the same arrangement but with the opposite orientation of the carboxamide moieties. The two constructs are hence termed $\mathbf{A_1}$**'** and $\mathbf{A_1}$**"**.

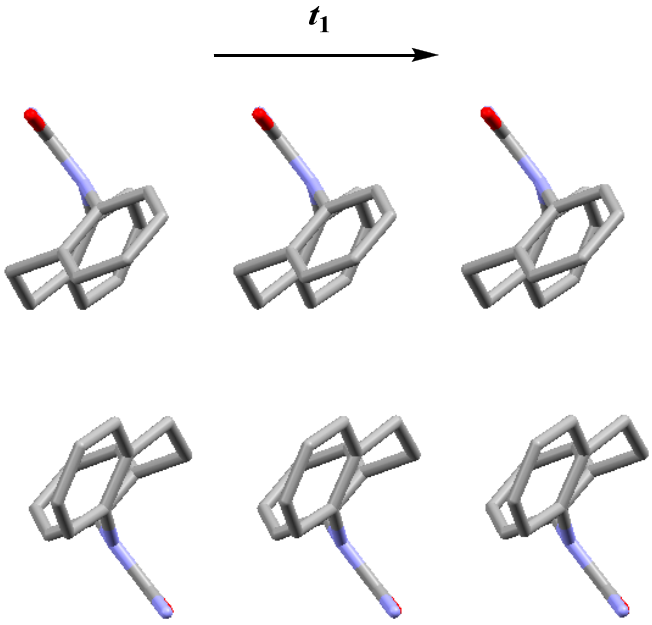

Figure S5a: 1-D construct $\mathbf{A_1}$**'** in **4**.

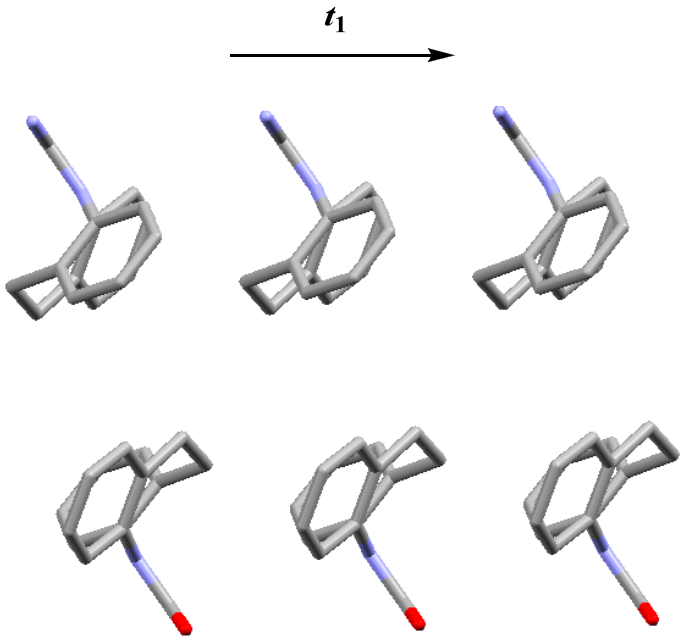

Fig S5b: 1-D construct **A$_1$"** in **1** and **3.**

Construct **B** is a hydrogen bonded catamer that occurs in structures **1**, **2** and **3** (fig. S6) and is absent from **4** where the structure is composed of hydrogen bonded *anti* dimers.

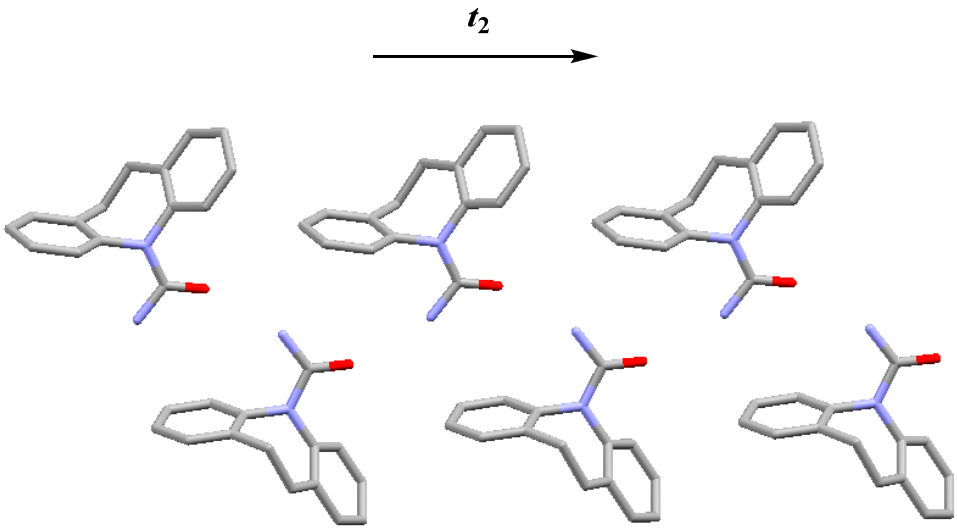

Fig. S6: Construct **B** viewed approximately perpendicular to translation vector t_2.

As stated previously in structures **1** and **3** the **A$_1$"** construct arises from the face-to-face stacking of these catamers along the t_1 vector. In **2** the catamers adopt a different arrangement along the equivalent axis (fig. S7). This arrangement can be described as a displaced stack along the crystallographic *b*-axis with alternating DHC molecules

displaced laterally by half a molecule along the a axis and out of plane with each other by an angle of 30°.

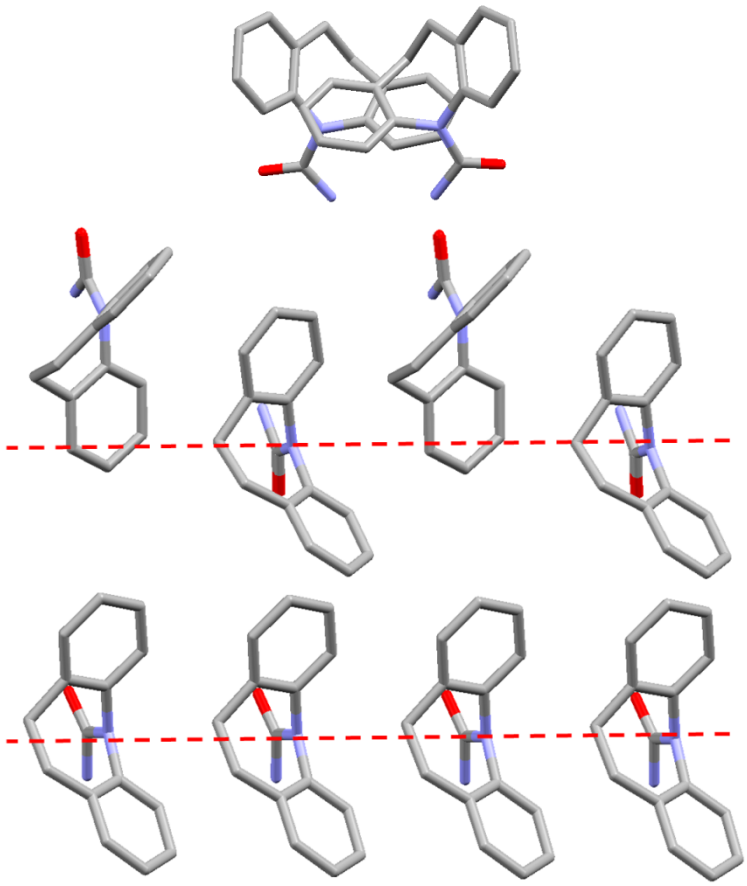

Fig S7: Displaced stacking arrangement in **2** viewed along b-axis (top) and approximately perpendicular to b (middle). The **A_1'** construct is shown for comparison (bottom). The dashed rd line indicates an axis through the centre of the carboxamide group.

The similarity relationships between the identified constructs are shown in Table S6 with the data for the base vectors in the constructs given in Table S7:

Table S6: Similarity relationships

SC	D	Description	Fig	Base	Dependencies
A	**1**	**Stack of molecules (translation)**	**1**	t_1	
A_1	**1**	**Double stack with two A strands related by inversion**	**2**	t_1	**A → A_1**
B	**1**	**Hydrogen bonded catamers**	**3**	t_2	
C	**3**	**A_1" stacks linked into B catamers**	**4**	t_1,t_2,t_3	**A_1 × B → C**

Table S7: Data for base vectors *t* in 1-D and 3-D SCs (lengths *d* in Å and angles in °)

Str	t_1	d_1	t_2	d_2	t_3	d_3	<(t_1,t_2)	<(t_1,t_3)	<(t_2,t_3)
1	**0-10**	**5.351**	**010**	**9.158**	**101**	**24.320**	**90**	**82.9**	**90**
2	**-**	**-**	**100**	**9.059**					
3	**100**	**5.423**	**0-10**	**9.200**	**10-1**	**24.252**	**91.1**	**82.9**	**87.8**
4	**100**	**5.505**							

In structures **1** and **3** the occurrence of both constructs leads to 3-dimensional similarity with the arrangement shown in fig S8. The structures are viewed parallel to the t_1 translation vector so each molecule represents an **A** stack, which propagate along the *a*-axis in both cases:

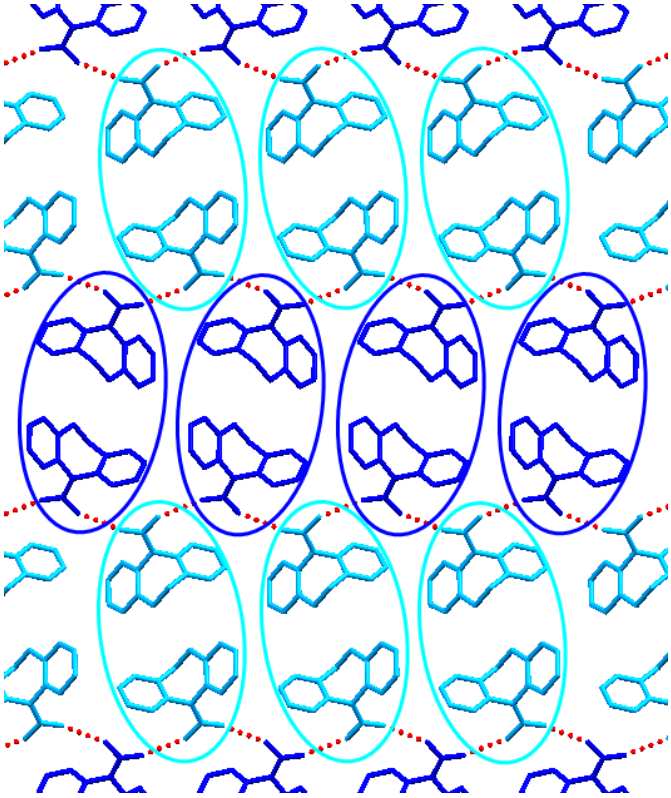

Fig S8. Packing of $\mathbf{A_1}$" constructs in **1** and **3**.

The packing arrangement of the $\mathbf{A_1}$ constructs is different in **4** (fig.S9) as a result of the different hydrogen bonding arrangement. In **1** and **3** the $\mathbf{A_1}$" constructs adopt a corrugated arrangement with alternating layers along the $\boldsymbol{t_2}$ vector offset from each other while in **4** they pack to form parallel layers.

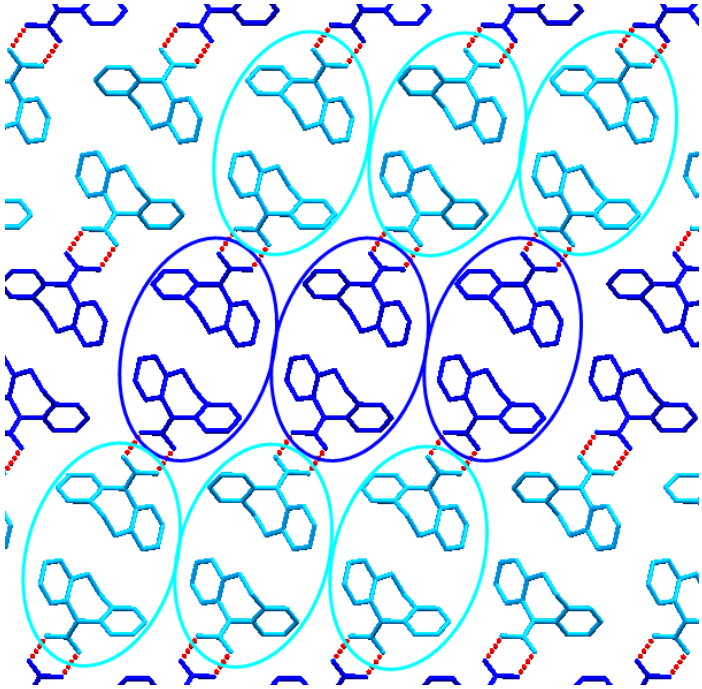

Fig S9. Packing of **A_1'** constructs in **4**.

The structural relationships between the four structures are further summarised in Figure 4 in the main manuscript.

4. Simulated XRPD Data for DHC Form IV

At the time of writing, no bulk samples of form IV were available to allow measurement of an experimental XRPD pattern or thermal properties via DSC. However, a calculated XRPD pattern for form IV DHC is provided in Fig S10.

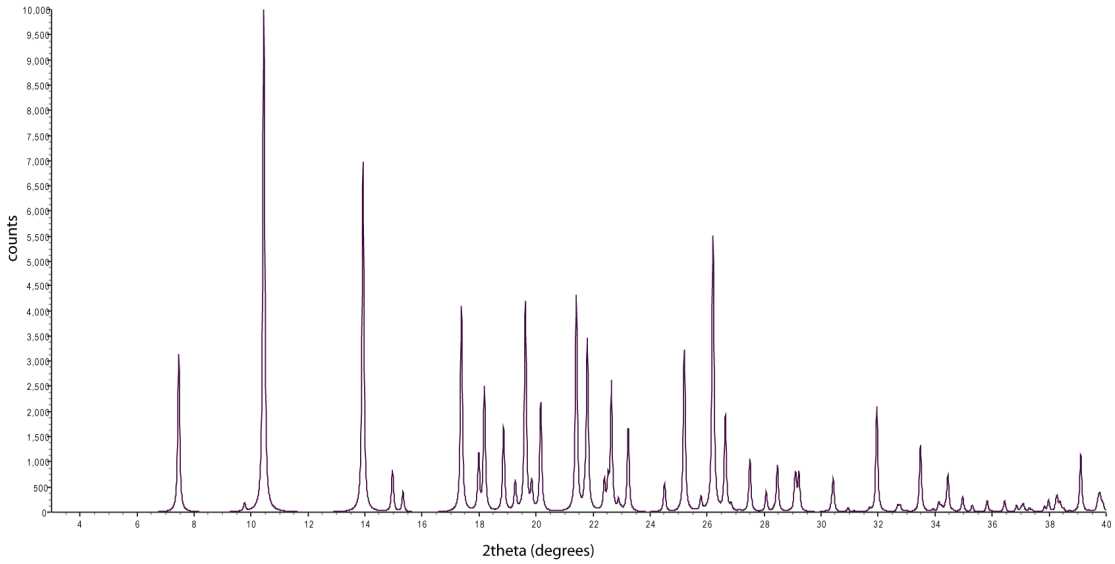

Fig S10. XRPD pattern calculated by Mercury for DHC form IV. Data calculcated in the range 3 – 40 $^{o}2\theta$ using λ = 1.54056 Å, FWHM = 0.08 $^{o}2\theta$.

References

Anghel, A. T.; Day, G. M.; Price, S. L. *CrystEngComm* **2002,** *4*, 348-355.
Bandoli, G., Nicolini, M., Ongaro, A., Volpe, G. & Rubello, A. (1992). *J. Chem. Crystallogr.* **22**, 177–183.
Coombes, D. S.; Price, S. L.; Willock, D. J.; Leslie, M. *J. Phys. Chem.* **1996,** 100, 7352-7360.
Florence, A. J.; Baumgartner, B.; Weston, C.; Shankland, N.; Kennedy, A. R.; Shankland, K.; David, W. I. F. *J. Pharm. Sci.* **2003,** *92,* 1930-1938.
Harrison, W. T. A., Yathirajan, H. S. & Anilkumar, H. G. (2006). *Acta Cryst.* C**62**, o240–o242.
Holden, J. R.; Du, Z. Y.; Ammon, H. L. *J.Comput.Chem.* **1993,** *14*, 422-437.
Johnston, A., Florence, A. J., Fernandes, P., Shankland, N., Kennedy, A. R. (2007) *Acta Cryst.* **E63**, o1469-o1470.
Johnston, A., Florence, A. J., Fernandes, P., Shankland, N., Kennedy, A. R. (2006) *Acta Cryst.* **E62**, o5361-o5362.
Johnston, A., Florence, A. J., Fernandes, P., Shankland, N., Kennedy, A. R. (2007) *Acta Cryst.* **E63**, o3888-o3889.
Johnston, A., Florence, A. J., Shankland, K., Leech, C. K., Shankland, N., Fernandes, P., (2007) *Acta Cryst.* **E63**, o3918-o3919.
Leech, C. K., Florence, A. J., Shankland, K., Shankland, N. & Johnston, A. (2007). *Acta Cryst.* **E63**, o675-o677.
Reboul J. P., Cristau B., Estienne J.and A. J. P., (1980) *Acta Cryst.*, **B36**, 2108-2112.
Willock, D. J.; Price, S. L.; Leslie, M.; Catlow, C. R. A. *J.Comput.Chem.* **1995,** *16*, 628-647**.**